Unexpected enhancement of ozone exposure and health risks during National Day in China

Peng Wang[1, 2], Juanyong Shen[3], Men Xia[1], Shida Sun[4], Yanli Zhang[2], Hongliang Zhang[5,6], Xinming Wang[2]

[1]Department of Civil and Environmental Engineering, The Hong Kong Polytechnic University, Hong Kong SAR, China

[2]State Key Laboratory of Organic Geochemistry and Guangdong Key Laboratory of Environmental Protection and Resources Utilization, Guangzhou Institute of Geochemistry, Chinese Academy of Sciences, Guangzhou, China

[3]School of Environmental Science and Engineering, Shanghai Jiao Tong University, Shanghai, China

[4]Tianjin Key Laboratory of Urban Transport Emission Research, College of Environmental Science and Engineering, Nankai University, Tianjin, China

[5]Department of Environmental Science and Engineering, Fudan University, Shanghai, China

[6]Institute of Eco-Chongming (IEC), Shanghai, China

Correspondence to: Yanli Zhang (zhang_yl86@gig.ac.cn)

Abstract

China is confronting increasing ozone (O_3) pollution that worsens air quality and public health. Extremely O_3 pollution occurs more frequently under special events and unfavorable meteorological conditions. Here we observed significantly elevated maximum daily 8-h average (MDA8) O_3 (up to 98 ppb) during the Chinese National Day Holidays (CNDH) in 2018 throughout China, with a prominent rise by up to 120% compared to the previous week. The air quality model shows that increased precursor emissions and regional transport are major contributors to the elevation. In the Pearl River Delta region, the regional transport contributed up to 30 ppb O_3 during the CNDH. Simultaneously, aggravated health risk occurs due to high O_3, inducing 33% additional deaths throughout China. Moreover, in tourist cities such as Sanya, daily mortality even increases significantly from 0.4 to 1.6. This is the first comprehensive study to investigate O_3 pollution during CNDH at the national level, aiming to arouse more focuses on the O_3 holiday impact from the public.

Graphical abstract

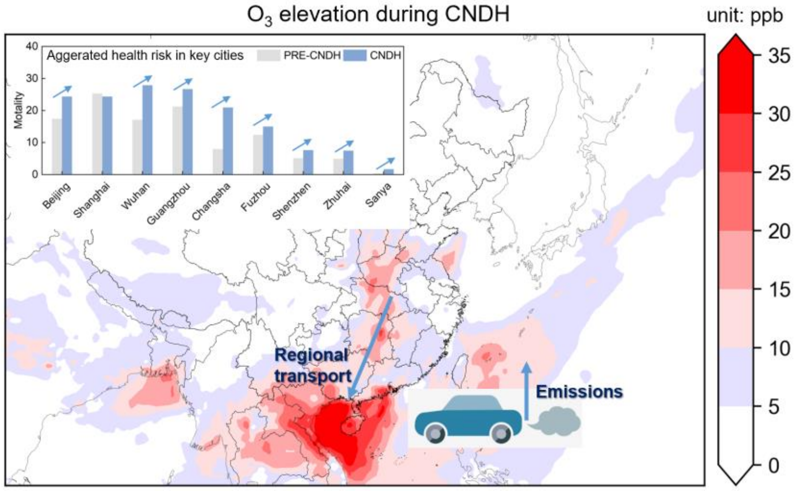

1. Introduction

Tropospheric ozone (O_3) has become a major air pollutant in China especially in urban areas such as the North China Plain (NCP), Yangtze River Delta (YRD) and Pearl River Delta (PRD) in recent years, with continuously increasing maximum daily 8-h average (MDA8) O_3 levels (Fang et al., 2019;Li et al., 2019;Lu et al., 2018;Liu et al., 2018a). Exacerbated O_3 pollution aggravates health risks from a series of illnesses such as cardiovascular diseases (CVD), respiratory diseases (RD), hypertension, stroke and chronic obstructive pulmonary disease (COPD) (Liu et al., 2018a;Li et al., 2015;Brauer et al., 2016;Lelieveld et al., 2013;Wang et al., 2020b). In China, the annual COPD mortality due to O_3 reaches up to 8.03×10^4 in 2015 (Liu et al., 2018a).

O_3 is generated by non-linear photochemical reactions of its precursors involving volatile organic compounds (VOCs) and nitrogen oxides (NO_x) (Sillman, 1995;Wang et al., 2017b). The VOCs/NO_x ratio determines O_3 sensitivity that is classified as VOC-limited, transition and NO_x-limited, which controls O_3 formation (Sillman, 1995;Sillman and He, 2002;Cohan et al., 2005). Also, regional transport was reported as an important source of high O_3 in China (Gao et al., 2016;Wang et al., 2020a;Li et al., 2012a). For instance, Li et al. (2012b) showed that over 50% of surface O_3 was contributed from regional transport in the PRD during high O_3 episodes.

O_3 concentration shows different patterns between holidays and workdays (Pudasainee et al., 2010;Xu et al., 2017). Elevated O_3 has been observed during holidays in different regions resulted from changes in precursor emissions related to intensive anthropogenic activities (Tan et al., 2009;Chen et al., 2019;Tan et al., 2013;Levy, 2013). In China, most studies focused on the Chinese New Year (CNY) to investigate long-term holiday effect on O_3 in southern areas (Chen et al., 2019). However, the Chinese National Day

Holidays (CNDH), a nationwide 7-day festival, is less concerned. Xu et al. (2017) reported that the O_3 production was influenced by enhanced VOCs during CNDH in the YRD based on in-situ observations. Previous studies mainly paid attention to developed regions/cities without nationwide consideration. In addition, the national O_3-attributable health impact during CNDH is also unclear. Consequently, a comprehensive study on O_3 during the CNDH is urgently needed in China.

In this study, we used observation data and a source-oriented version of the Community Multiscale Air Quality (CMAQ) model (Wang et al., 2019b) to investigate O_3 characteristics during the CNDH in 2018 in China. Daily premature death mortality was evaluated to determine health impacts attributed to O_3 as well. We find a rapid increase by up to 120% of the observational MDA8 O_3 from previous periods to CNDH throughout China, which is attributed to increased precursors and regional transport. This study provides an in-depth investigation of elevated O_3 and its adverse health impacts during CNDH, which has important implications for developing effective control policies in China.

2. Methods

2.1 The CMAQ model setup and validation

The CMAQ model with three-regime (3R) attributed O_3 to NO_x and VOCs based on the NO_x-VOC-O_3 sensitivity regime was applied to study the O_3 during CNDH in China in 2018. The regime indicator R was calculated using Eq. (1):

$$\mathrm{R} = \frac{P_{H_2O_2} + P_{ROOH}}{P_{HNO_3}} \tag{1}$$

where $P_{H_2O_2}$ is the formation rate of hydrogen peroxide (H_2O_2); P_{ROOH} is the formation rate of organic peroxide (ROOH), and P_{HNO_3} is the formation rate of nitric acid (HNO_3) in each chemistry time step. The threshold values for the transition regime are 0.047 (R_{ts}, change from VOC-limited to transition regime) and 5.142 (R_{te}, change from transition regime to NO_x-limited regime) in this study (Wang et al., 2019a). The formed O_3 is entirely attributed to NO_x or VOC sources, when R values are located in NO_x-limited ($R>R_{te}$) or VOC-limited ($R<R_{ts}$) regime. In contrast, when R values are in the transition regime ($R_{ts} \leq R \leq R_{te}$), the formed O_3 is attributed to both NO_x and VOC sources. Two non-reactive O_3 species: O_3_NO_x and O_3_VOC are added in the CMAQ model to quantify the O_3 attributable to NO_x and VOCs, respectively. In particular, O_3_NO_x stands for the O_3 formation is under NO_x -limited control, and O_3_VOC stands for the O_3 formation is under VOC-limited control. The details of the 3R scheme and the calculation of O_3_NOx and O_3_VOC are described in Wang et al. (2019a). A domain with a horizontal resolution of 36×36 km^2 was applied in this study, covering China and its surrounding areas (Fig. S1). Weather Research and Forecasting (WRF) model version 3.9.1 was used to generate the meteorological inputs, and the initial and

boundary conditions were based on the FNL reanalysis data from the National Centers for Environmental Prediction (NCEP). The anthropogenic emissions in China are from the Multiresolution Emission Inventory for China (MEIC, http://www.meicmodel.org/) version 1.3 that lumped into 5 sectors: agriculture, industries, residential, power plants, and transportation. The annual MEIC emission inventory was applied in this study and the monthly profile of the anthropogenic emissions was based on Zhang et al. (2007) and Streets et al. (2003) as shown in Table S1 to represent the emissions changes between September and October. The higher emissions rates were found during October from the residential and industrial sectors, while they kept the identical levels from transportation and power sectors. Emissions from other countries were from MIX Asian emission inventory (Li et al., 2017). Open burning emissions were from the Fire INventory from NCAR (FINN) (Wiedinmyer et al., 2011), and biogenic emissions are generated using the Model of Emissions of Gases and Aerosols from Nature version 2.1 (MEGAN2.1) (Guenther et al., 2012). The Integrated Process Rate (IPR) in the Process Analysis (PA) tool in the CMAQ model was applied to quantify the contributions of atmospheric processes to O_3 (Gipson, 1999) (details see Table S2). In the CMAQ model, the IPR and integrated reaction rate analysis (IRR) were all defined as the PA. PA aims to provide quantitative information on the process of the chemical reactions and other atmospheric processes that are being simulated, illustrating how the CMAQ model calculated its predictions. The IPR was used to determine the relative contributions of individual atmospheric physical and chemical processes in the CMAQ model.

The simulation period was from 24 September to 31 October in 2018 and divided into three intervals: PRE-CNDH (24-30, September), CNDH (1-7, October) and AFT-CNDH (8-31, October). In this study, a total of 43 cities includes both megacities (such as Beijing and Shanghai) and popular tourist cities (such as Sanya), were selected to investigate the O_3 issue during CNDH in 2018 in China (Table S3). Locations of these cities cover developed (such as the YRD region) and also suburban/rural regions (such as Urumqi and Lhasa in western China), which provides comprehensive perspectives for this study (Fig. S1).

All the statistics results of the WRF model are satisfied with the benchmarks (Emery et al., 2001) except for the GE of temperature (T2) and wind speed (WD) went beyond the benchmark by 25% and 46%, respectively (Table S4). The WRF model performance is similar to previous studies (Zhang et al., 2012;Hu et al., 2016) that could provide robust meteorological inputs to the CMAQ model. The observation data of key pollutants obtained from the national air quality monitoring network (https://quotsoft.net/air/, more than 1500 sites) were used to validate the CMAQ model performance. The model performance of O_3 was within the criteria (EPA, 2005) with a slight underestimation compared to observations, demonstrating our simulation is capable of the O_3 study in China (Table S5).

2.2 Health impact estimation

The daily premature mortalities due to O_3 from all non-accidental causes, CVD, RD, hypertension, stroke and COPD are estimated in this study. The O_3-related daily mortality is calculated based on Anenberg et al. (2010) and Cohen et al. (2004). In this study, the population data are from all age groups, which may induce higher daily mortality than expected (Liu et al., 2018a). In this study, the daily premature mortality due to O_3 is calculated from the following Eq. (2) (Anenberg et al., 2010;Cohen et al., 2004) :

$$\Delta M = y_0[1 - exp(-\beta \Delta X)]Pop \quad (2)$$

where ΔM is the daily premature mortality due to O_3; y_0 is the daily baseline mortality rate, collected from the China Health Statistical Yearbook 2018 (National, 2018); β is the concentration-response function (CRF), which represents the increase in daily mortality with each 10 μg m^{-3} increase of MDA8 O_3 concentration, cited from Yin et al. (2017); ΔX is the incremental concentration of O_3 based on the threshold concentration (35.1 ppb) (Lim et al., 2012;Liu et al., 2018a); *Pop* is the population exposure to O_3, obtained from China's Sixth Census data (Fig. S2) (National Bureau of Statistics of China, 2010). The daily y_0 and β values for all non-accidental causes, CVD, RD, hypertension, stroke and COPD are summarized in Table S6.

3. Results and Discussions

3.1 Observational O_3 in China during CNDH

MDA8 O_3 levels have noticeably risen during the 2018 CNDH based on observations, from 43 ppb (PRE-CNDH) to 55 ppb (CNDH) among selected cities (Fig. 1a and Table S3). The most significant increase of MDA8 O_3 (up to 56%) is observed in South China (Fig. 1b). The PRD region has recorded 49 % of MDA8 O_3 increase, and in most PRD cities (such as Shenzhen and Guangzhou), the number of exceeding days is as high as 5~7 days during the 7-day CNDH, which contributed to 50 ~ 86% of days exceeding the Chinese national air quality standards (Grade II, ~75 ppb) in the whole October (Fig. 1c). Other regions exhibit less MDA8 O_3 increases, which are 20%, 16% and 3% for East, North and West China, respectively (Fig. 1b). Negligible MDA8 O_3 increase in West China is consistent with vast rural areas and less anthropogenic impacts (Wang et al., 2017a). This result suggests that changes in anthropogenic emissions have significant impacts on MDA8 O_3 during the CNDH in South, East, and North China, similar to a previous observation study (Xu et al., 2017).

Nine key cities are then selected for analyzing the causes and impacts of the remarkable MDA8 O_3 rises. Comprehensive criteria were adopted in selection according to: (1) acute MDA8 O_3 increases (e.g., Changsha and Shenzhen), and (2) important provincial capitals (e.g., Beijing and Shanghai) and famous tourist cities (e.g., Sanya). The selected key cities are delegates of broad regions in China except for West

China (Fig. S1), which has an insignificant MDA8 O_3 increase (Table S3) and fewer traveling cities. The MDA8 O_3 increased by 48±37 % during the 2018 CNDH in these key cities. The highest MDA8 O_3 is observed in Zhuhai, reaching 98 ppb on average with the peak of 107 ppb. The MDA8 O_3 in Sanya increases twofold compared to PRE-CNDH, which is unexpected because Sanya is less concerned about air pollution and is known for less anthropogenic emissions (Wang et al., 2015). Other key cities show 8-70 % increases during the CNDH. The exact causes of substantial O_3 increases in these cities are of high interest and explored below.

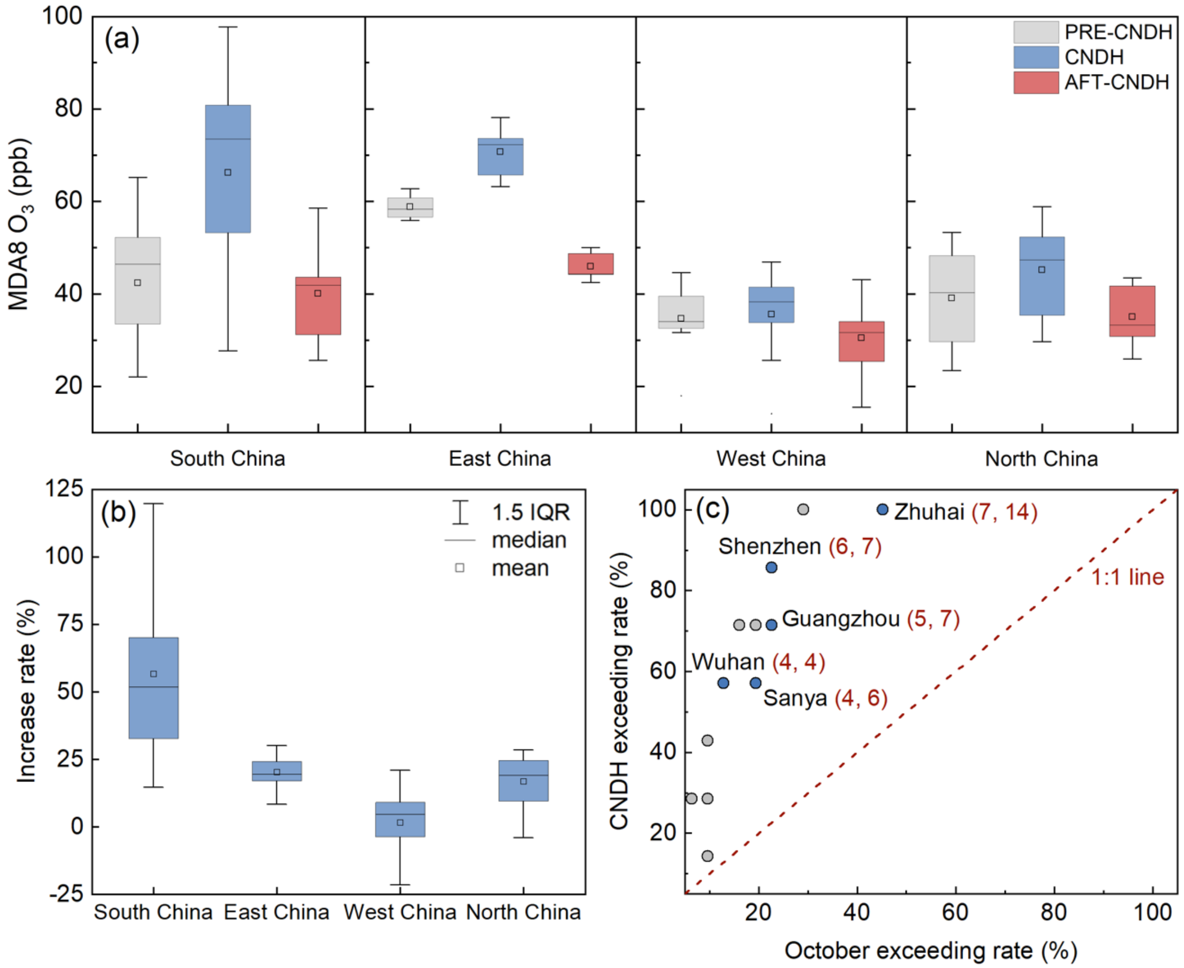

Figure 1. (a) The observed average MDA8 O_3 in PRE-CNDH, CNDH and AFT-CNDH in South, East, West and North China in 2018; **(b)** The increase rate of observed MDA8 O_3 during CNDH; **(c)** The exceeding rate of observed MDA8 O_3 in CNDH and October (the exceeding days during the CNDH divided by that during the October, exceeding_CNDH/exceeding_October). Locations of these regions are shown in Fig. S3. Blue dots refer to the key cities and grey dots represent other cities. The pairs of values in the parentheses following city name are the exceeding days in CNDH and October, respectively. IQR is the interquartile range.

3.2 Increased O_3 precursor emissions during CNDH

The CMAQ is capable to represent the changes in observed MDA8 O_3 (Fig. 2). Generally, increasing trends of MDA8 O_3 are found in vast areas from PRE-CNDH to CNDH, suggesting the elevated O_3 occurs on a regional-scale. In South China, the predicted MDA8 O_3 reaches ~90 ppb that is approximately 1.2 times of the Class II standard with an average increase rate of 30%. The highest MDA8 O_3 drops sharply to 60 ppb in the same regions in AFT-CNDH. High O_3_NO_x and O_3_VOC levels are also found during CNDH with different spatial distributions (Fig. 2). The rising O_3_NO_x areas are mainly located in South China, covering Hubei, Hunan, Guangxi, Jiangxi, north Guangdong, and Fujian provinces with an average increase of ~5-10 ppb. In contrast, high O_3_VOC regions are in developed city clusters such as the NCP, YRD and PRD regions. In the PRD, peak O_3_VOC is over 30 ppb during the CNDH, which is 1.5 times of that in PRE-CNDH. Similar to MDA8 O_3, decreases in both O_3_NO_x and O_3_VOC are found in AFT-CNDH. For the nine key cities, O_3_NO_x and O_3_VOC are also increased during CNDH. In Sanya, non-background O_3 during CNDH is two times of that in PRE-AFDH. The peak of non-background O_3 (O_3_NO_x + O_3_VOC) is over 80 ppb in Beijing and Zhuhai, indicating that O_3 formation plays an important role during CNDH (Fig. 3). In megacities such as Beijing, O_3_VOC is the major contributor to elevated O_3, while O_3_NO_x becomes significant in tourist cities such as Sanya.

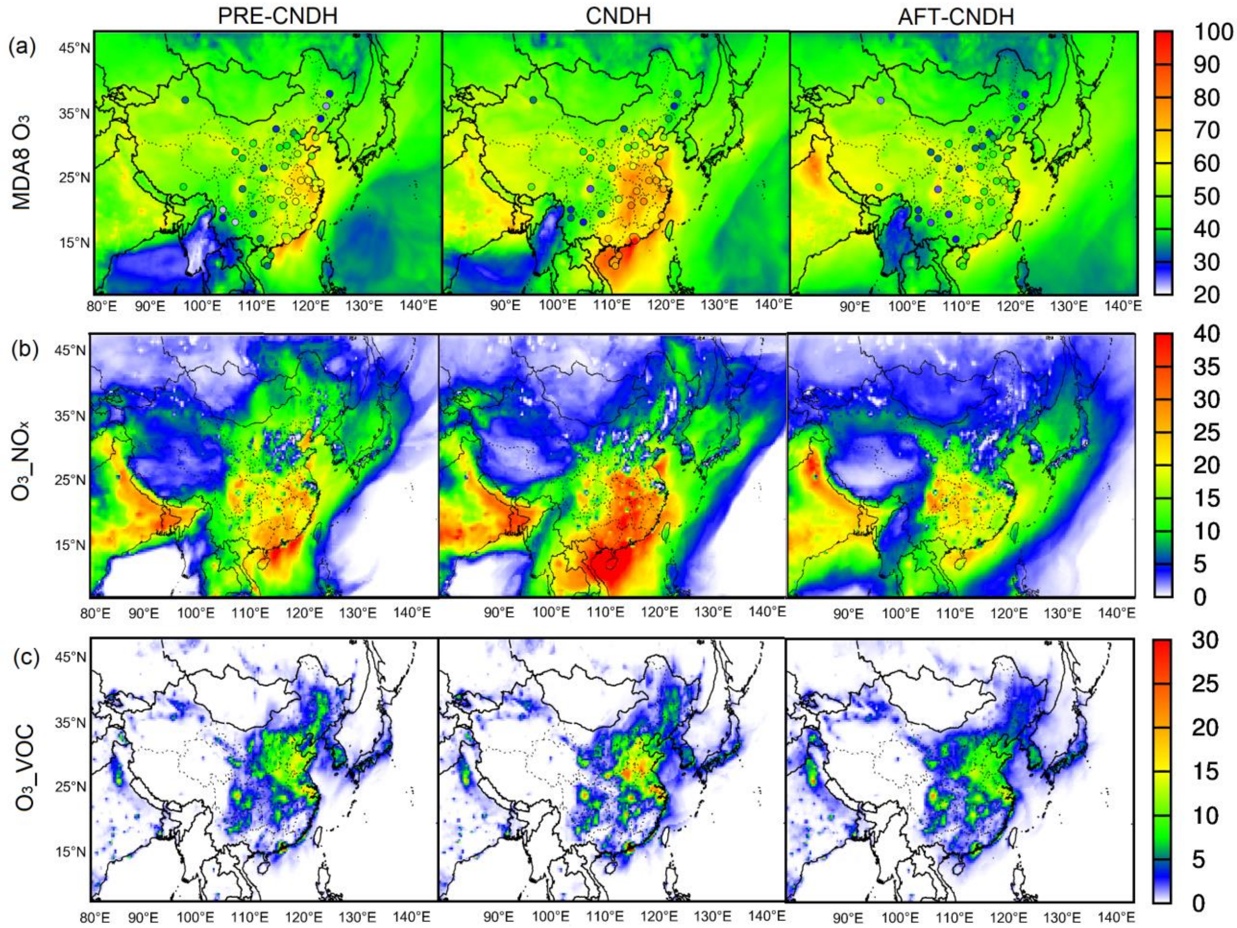

Figure 2. (a) Comparison of observed (circle) and predicted MDA8 O_3; **(b)** Spatial distribution of O_3_NO_x; **(c)** Spatial distribution of O_3_VOC in China in PRE-CNDH, CNDH and AFT-CNDH, respectively. Units are ppb. O_3_NO_x and O_3_VOC are the O_3 attributed to NO_x and VOCs, respectively.

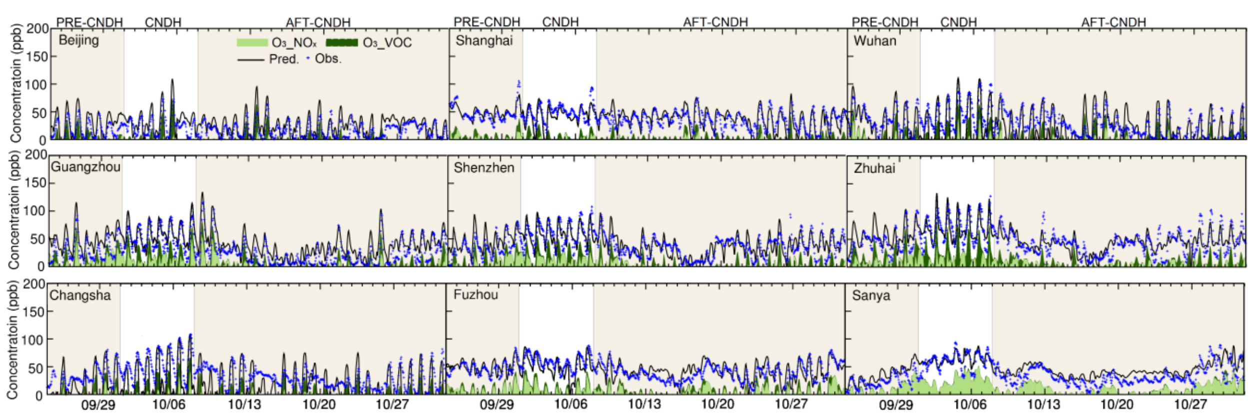

Figure 3. Hourly O_3 and its source apportionment results in nine key cities.

From Figure 4, the anthropogenic O_3 precursor emissions (NO_x and VOCs) increase throughout China. Increasing NO_x emissions are observed in South China, especially in Guangxi and Guangdong, with a relative increase of up to 100% during CNDH. Considering O_3 sensitivity regimes (determined by Eq. (1)), no noticeable differences are observed between PRE-CNDH and CNDH (Fig. S4). During CNDH, the VOC-limited regions are mainly in the NCP and YRD accompanied by high O_3_VOC. In South China, O_3 formation is under a transition regime in most regions, and NO_x-limited areas are in Fujian and part of Guangdong and Guangxi where have rising NO_x emissions. This is corresponding to an increasing in O_3 in these regions (Fig. 2 and Fig. 4). Simultaneously, higher anthropogenic VOC emissions are also observed during CNDH in South China, leading to elevated O_3 in the transition regime when VOCs and NO_x jointly controlled O_3 formation. These increasing O_3 precursors emissions are mainly from the residential and transportation sectors (Table S1), indicating their important roles in the elevated O_3 during the CNDH. In contrast, during AFT-CNDH, more areas turn into a transition regime in South China. The decreases in biogenic VOCs (BVOCs, compared to CNDH) (Fig. 4) due to temperature (Fig. S5) decrease MDA8 O_3 for regions in transition regime during AFT-CNDH. Accordingly, changes in O_3 highly depend on its precursor (NO_x and VOCs) emissions and the sensitivity regime.

Transportation increase due to tourism is also a potential source of elevated O_3 during holidays (Xu et al., 2017). However, changes in transportation emissions are not considered in this study due to a lack of related statistical data. Residents prefer to travel during CNDH, and thus more significant impacts may be from mobile sources (Zhao et al., 2019). Traveling by private cars is the most common approach, leading to a significant increase in vehicle activities (Wang et al., 2019c). Time-varying coefficients are estimated to describe traffic flow according to AMAP (2018) report during 2018 CNDH (Fig. S6). On average, CNDH is 2.2 times the traffic flow of ordinary weeks. The heavy traffic flow occurs on October 1st (coefficient of 16.3%) and October 5th (6.1%) due to intensive departure and return. Hourly variations of traffic flow in CNDH are similar to weekends, having a flatter trend compared to workdays (Liu et al., 2018b). A real-time vehicle emission inventory should be developed in future to better predict O_3 changes during CNDH.

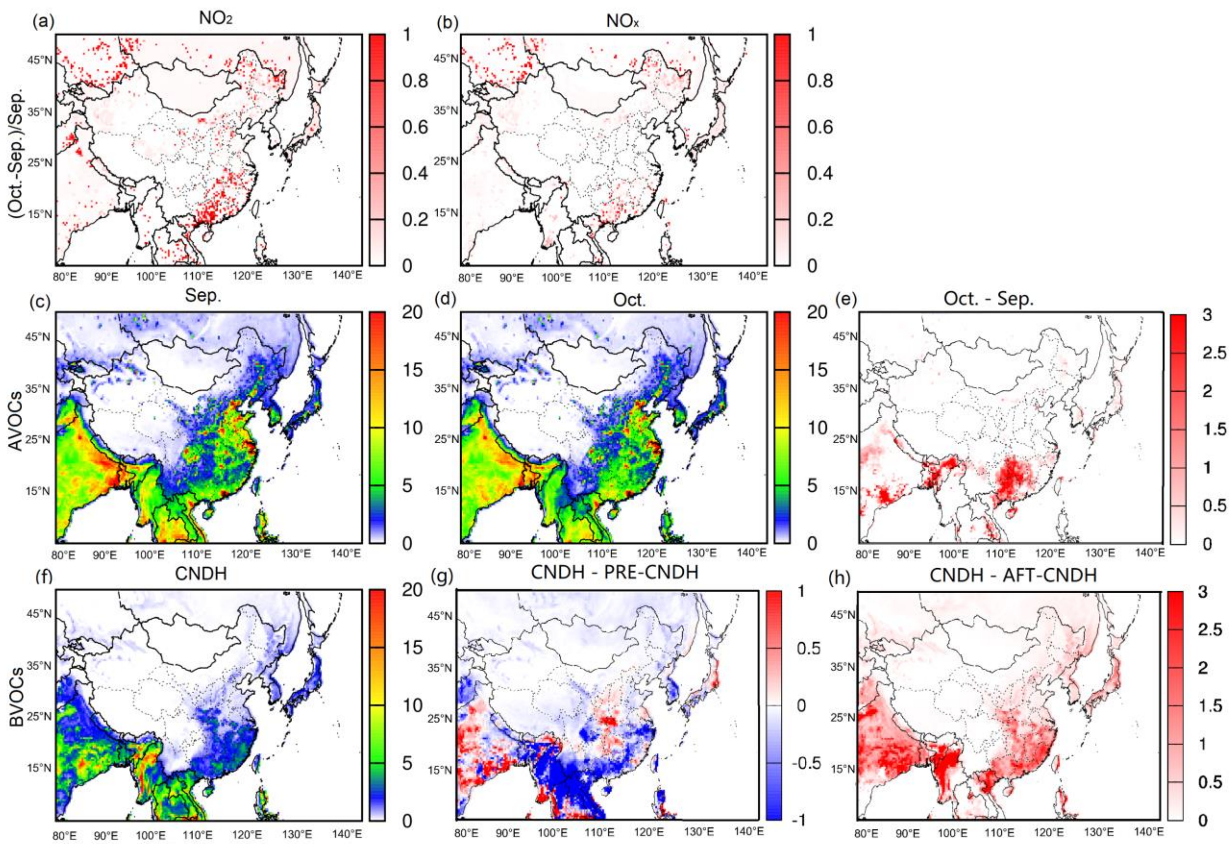

Figure 4. Changes of emissions in relative differences ((Oct.-Sep.)/Sep.) of **(a)** NO_2 and **(b)** NO_x. Averaged emissions rates of AVOCs from MEIC emission inventory in **(c)** September and **(d)** October and their difference **(e)**. Averaged BVOCs emission rates from the MEGAN model in **(f)** CNDH and their differences **(g)** CNDH subtracts PRD-CNDH and **(h)** CNDH subtracts AFT-CNDH. Units are moles/s for (c)-(h).

3.3 Impacts of regional Transport during CNDH

Regional transport is also a significant contributor to enhanced MDA8 O_3 during CNDH. As shown in Fig. S5, the lower temperature is predicted during the CNDH compared to the PRE-CNDH. In PRD, the average temperature drops from 25 °C to 23 °C, leading to a lower O_3 level in previous studies (Fu et al., 2015;Bloomer et al., 2009;Pusede et al., 2015). Meanwhile, the increasing wind speed is predicted in the PRD, which is able to facilitate regional transport. The higher O_3 production rates that are calculated by the PA process directly in the CMAQ model (increase rate up to ~150%) are predicted mainly in the urban regions (the NCP, YRD, and PRD) in China (Fig. S7). With north winds (Fig. S5), O_3 is transported from the northern regions to downwind southern China to cause aggravated O_3. In the nine key cites, enhanced regional transport (HADV: horizontal advection) of O_3 in Beijing, Changsha, Fuzhou, Shenzhen, Sanya, and Shanghai is as high as 90 ppb (Fig. S8). The enhanced regional transport and the increasing anthropogenic emissions synergistically lead to the rising O_3 during the CNDH, offsetting the impacts from the lower BVOCs emissions (Fig. 4).

A regional-source tracking simulation was conducted in the PRD that occurred significant O_3 elevation to qualify the impacts of regional transport. The emissions were classified into seven regional types (Fig. S9): the local PRD (GD), northern part (NOR), southern part (SOU), central part (CEN), western part (WES), southeast part (SWE), and other countries (OTH). The detailed model description could be found in Wang et al. (2020a). Although the local sector contributes more than 50% non-background O_3 from PRE-CNDH to AFT-CNDH, the more significant O_3 regional transport is predicted during the late PRE-CHDH and CNDH in the PRD, manifesting its important role in the O_3 elevation (Fig. 5 and Fig. S10). The SOU sector is the most crucial contributor among all these regional sectors outside Guangdong due to the prevailing north wind.

In these PRD key cities (Guangzhou, Shenzhen, and Zhuhai), the contribution of SOU sector in the non-background O_3 is up to ~30 ppb, mainly occurring in the nighttime and early morning (Fig. 5). In the noontime, ~10-15% non-background O_3 is from the SOU sector during the CNDH compared to less than 5% in other periods. The O_3_NO_x shows more significant regional transport characteristics than the O_3_VOC (Fig. S11 and Fig. S12). During the late pre-CNDH and the CNDH, the contribution from regional transport in the O_3_NO_x is up to 35 ppb. Due to the enhanced regional transport during the CNDH, the O_3_NO_x could be even transported from the long-distance sector as NOR to the PRD. The peak of O_3_NO_x due to the regional transport is predicted at midnight, which is different from O_3_VOC (peak at noontime).

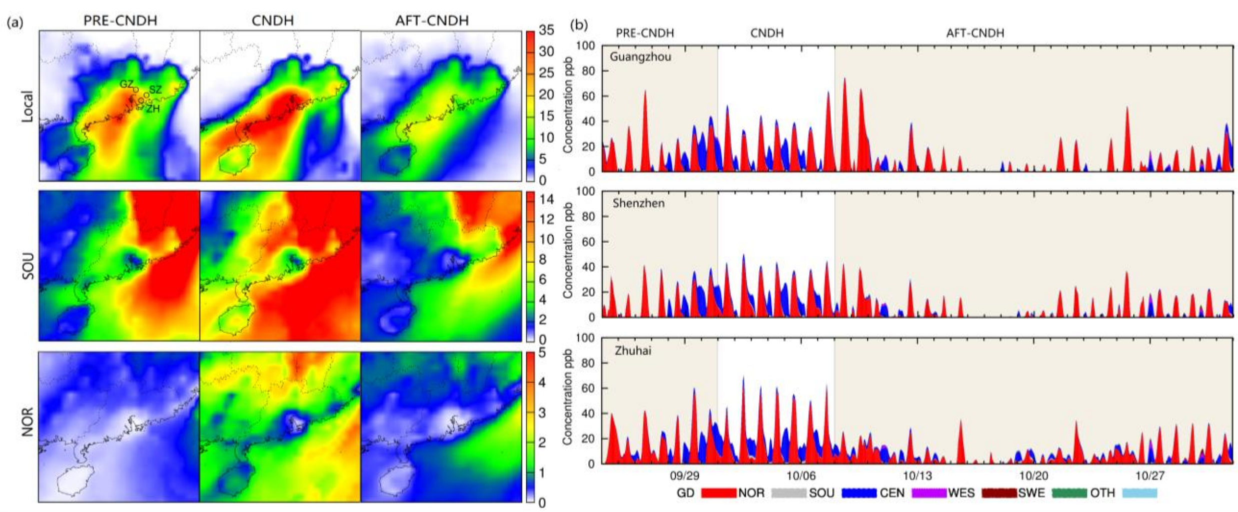

Figure 5. (a) Average regional contributions to non-background O_3 from the PRD local emissions and emissions in SOU, and NOR sectors and **(b)** regional contributions from all sectors to non-background O_3

in the PRD key cities (Guangzhou, Shenzhen, and Zhuhai) during the simulation periods. GZ: Guangzhou, SZ: Shenzhen, and ZH: Zhuhai.

3.4 Aggravated Health Risk during CNDH

It is recognized that O_3 pollution induces serious health risks from CVD, RD, COPD, hypertension, and stroke (Lelieveld et al., 2013;Yin et al., 2017;Huang et al., 2018;Krewski et al., 2009). Elevated MDA8 O_3 during CNDH leads to significantly higher health risks (Fig. 6). The estimated total national daily mortality (from all non-accidental causes) due to MDA8 O_3 is 2629 during CNDH, 33% higher than that (1982) in PRE-CNDH. All above O_3-related diseases have noticeable increases in national daily mortality during CNDH. The highest health risk among these diseases is from CVD (674 during the CNDH), which is consistent with Yin et al. (2017), followed by RD (219), COPD (213), hypertension (189), and stroke (22). The COPD mortality due to O_3 in this study is comparable with 152-220 in Liu et al. (2018a). In AFT-CNDH, total daily mortality (drops to 1653) and mortality from all diseases decreases due to substantial O_3 reduction. Also, a significant increase of the total daily mortality is shown throughout China during the CNDH, especially in those densely-populated regions (e.g., the YRD and PRD) (Fig. S11), which is consistent with previous studies (Chen et al., 2018;Liu et al., 2018a;Wang et al., 2020b).

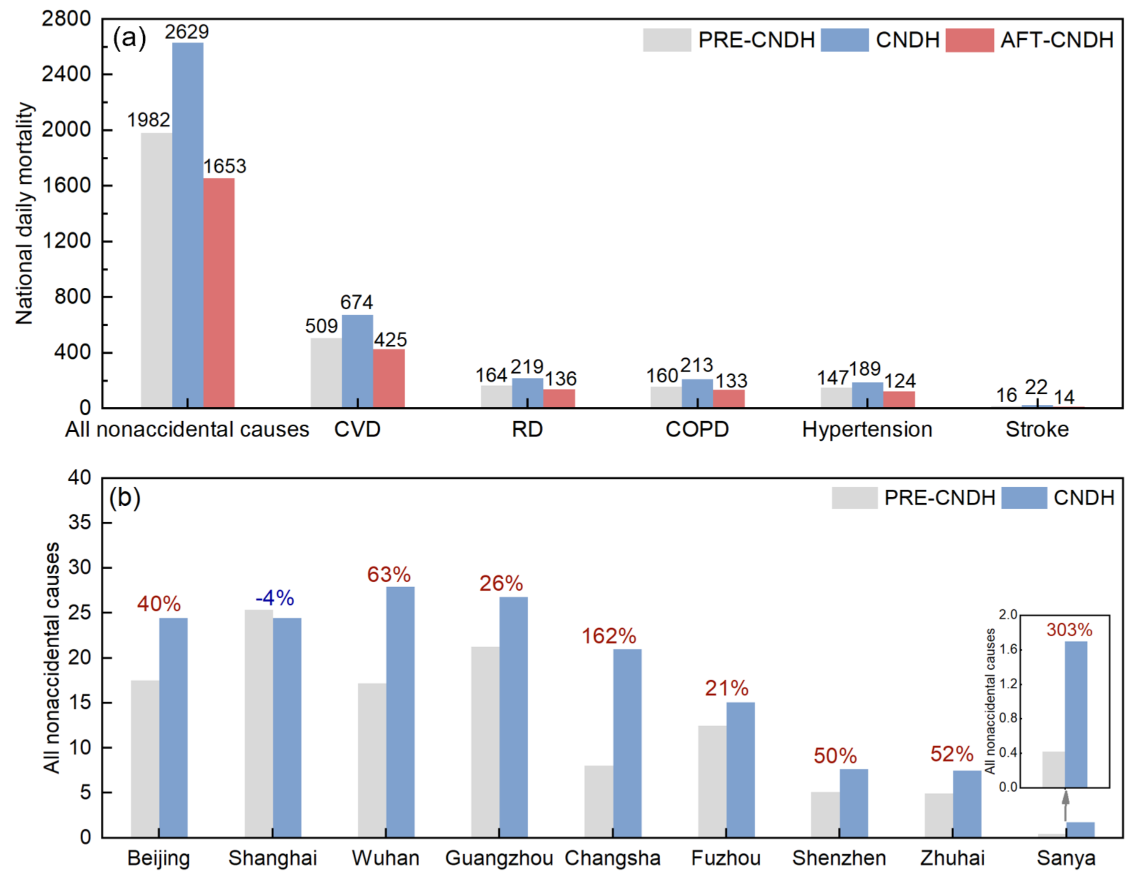

Figure 6. (a) National daily mortality from all non-accidental causes, CVD, RD, COPD, hypertension, and stroke attributed to O_3 in PRE-CDNH, CNDH, and AFT-CNDH and **(b)** Daily mortality from all non-accidental causes due to O_3 in the nine key cities. Red/blue values above the bars are the increase/decrease rates of daily mortality from PRE-CNDH to CNDH. CVD: cardiovascular diseases; RD: respiratory diseases; COPD: chronic obstructive pulmonary disease.

Except for Shanghai (in which O_3 is slightly underestimated), the other eight key cities increased their total daily mortality rates from PRE-CNDH to CNDH. Four megacities (Beijing, Shanghai, Wuhan and Guangzhou) with enormous populations have the highest daily deaths (24-28) during CNDH, 50% larger than the mean level (16) in the other 272 Chinese cities (Chen et al., 2018;Yin et al., 2017). It is worth noting that a higher increase rate of daily mortality is found in tourist cities (Sanya and Changsha). In Sanya, daily deaths even increase by as high as 303% from PRE-CNDH to CNDH. An even higher increase in health risk may occur in Sanya if considered a sharp increase in tourist flow during CNDH.

4. Conclusion and Implications

In this study, we find a significant increase in O_3 during the CNDH throughout China, especially in the south part, which is attributed to the changes in precursor emissions, sensitivity regime, and enhanced regional transport. Moreover, the elevated O_3 also causes severe impacts on human health, with total daily mortality from all non-accidental causes increasing from 151 to 201 in China. More comprehensive studies should be conducted to understand better the long-holiday impacts (such as during the CNDH) of O_3 in the future and here we suggest:

1) More strident emission control policies should be implemented in China before and during CNDH to inhibit the elevated O_3. And more localized control policies with the consideration of the O_3 sensitivity regimes should be applied.

2) For reducing the health risk from the elevated O_3, it is suggested to avoid traveling in rush hours, especially at midday during the CNDH.

3) Reducing the activities of private gasoline vehicles is effective in mitigating excess emissions during the CNDH. It is encouraged to go out by electric car or public transportation such as bus, subway, and train.

Acknowledgments. This work was supported by the National Natural Science Foundation of China (42022023/41961144029), the National Key Research and Development Program (2017YFC02122802), the Chinese Academy of Sciences (XDA23020301/QYZDJ-SSW-DQC032), the Hong Kong Research Grants Council (T24-504/17-N/A-PolyU502/16), Youth Innovation Promotion Association, CAS (2017406) and Guangdong Foundation for Program of Science and Technology Research (2020B1212060053).

Author contributions. PW and YZ designed the research. PW, JS, MX, SS and HZ analyzed the data. PW performed air quality model. PW and YZ wrote the manuscript with comments from all co-authors.

Competing interests. The authors declare that they have no conflict of interest.

Data availability. The datasets used in the study can be accessed from websites listed in the references or by contacting the corresponding author (zhang_yl86@gig.ac.cn).

References

Forecast report on travel index during Mid-Autumn Festival and National Day in 2018, 2018.

Anenberg, S. C., Horowitz, L. W., Tong, D. Q., and West, J. J.: An Estimate of the Global Burden of Anthropogenic Ozone and Fine Particulate Matter on Premature Human Mortality Using Atmospheric Modeling, Environmental Health Perspectives, 118, 1189-1195, 2010.

Bloomer, B. J., Stehr, J. W., Piety, C. A., Salawitch, R. J., and Dickerson, R. R.: Observed relationships of ozone air pollution with temperature and emissions, Geophysical Research Letters, 36, 2009.

Brauer, M., Freedman, G., Frostad, J., Van Donkelaar, A., Martin, R. V., Dentener, F., Van Dingenen, R., Estep, K., Amini, H., and Apte, J. S.: Ambient Air Pollution Exposure Estimation for the Global Burden of Disease 2013, Environmental Science & Technology, 50, 79-88, 2016.

Chen, K., Fiore, A. M., Chen, R., Jiang, L., Jones, B., Schneider, A., Peters, A., Bi, J., Kan, H., and Kinney, P. L.: Future ozone-related acute excess mortality under climate and population change scenarios in China: A modeling study, PLOS Medicine, 15, 2018.

Chen, P., Tan, P., Chou, C. C. K., Lin, Y., Chen, W., and Shiu, C.: Impacts of holiday characteristics and number of vacation days on “holiday effect” in Taipei: Implications on ozone control strategies, Atmospheric Environment, 202, 357-369, 2019.

Cohan, D. S., Hakami, A., Hu, Y., and Russell, A. G.: Nonlinear response of ozone to emissions: source apportionment and sensitivity analysis, Environmental Science & Technology, 39, 6739-6748, 2005.

Cohen, A. J., Anderson, H. R., Ostro, B., Pandey, K. D., Krzyzanowski, M., K¨unzli, N., Gutschmidt, K., Pope, A., Romieu, I., Samet, J. M., and Smith, K.: Urban air pollution, in: Comparative quantification of health risks, Global and regional burden of disease attributable to selected major risk factors, Volume 1, World Health Organization, Geneva, 2004.

Emery, C., Tai, E., and Yarwood, G.: Enhanced meteorological modeling and performance evaluation for two Texas ozone episodes, Prepared for the Texas natural resource conservation commission, by ENVIRON International Corporation, 2001.

EPA, U.: Guidance on the Use of Models and Other Analyses in Attainment Demonstrations for the 8-hour Ozone NAAQS, EPA-454/R-05-002, 2005.

Fang, X., Park, S., Saito, T., Tunnicliffe, R., Ganesan, A. L., Rigby, M., Li, S., Yokouchi, Y., Fraser, P. J., and Harth, C. M.: Rapid increase in ozone-depleting chloroform emissions from China, Nature Geoscience, 12, 89-93, 2019.

Fu, T.-M., Zheng, Y., Paulot, F., Mao, J., and Yantosca, R. M.: Positive but variable sensitivity of August surface ozone to large-scale warming in the southeast United States, Nature Climate Change, 5, 454-458, 2015.

Gao, J., Zhu, B., Xiao, H., Kang, H., Hou, X., and Shao, P.: A case study of surface ozone source apportionment during a high concentration episode, under frequent shifting wind conditions over the Yangtze River Delta, China, Science of The Total Environment, 544, 853-863, https://doi.org/10.1016/j.scitotenv.2015.12.039, 2016.

Gipson, G. L.: Chapter 16: Process analysis. In science algorithms of the EPA models-3 Community Multiscale Air Quality (CMAQ) Modeling System. EPA/600/R-99/030, 1999.

Guenther, A. B., Jiang, X., Heald, C. L., Sakulyanontvittaya, T., Duhl, T., Emmons, L. K., and Wang, X.: The Model of Emissions of Gases and Aerosols from Nature version 2.1 (MEGAN2.1): an extended and updated framework for modeling biogenic emissions, Geoscientific Model Development (GMD), 5, 1471-1492, 2012.

Hu, J., Chen, J., Ying, Q., and Zhang, H.: One-year simulation of ozone and particulate matter in China using WRF/CMAQ modeling system, Atmos. Chem. Phys., 16, 10333-10350, 10.5194/acp-16-10333-2016, 2016.

Huang, J., Pan, X., Guo, X., and Li, G.: Health impact of China's Air Pollution Prevention and Control Action Plan: an analysis of national air quality monitoring and mortality data, The Lancet Planetary Health, 2, 2018.

Krewski, D., Jerrett, M., Burnett, R. T., Ma, R., Hughes, E., Shi, Y., Turner, M. C., Pope, C. A., 3rd, Thurston, G., Calle, E. E., Thun, M. J., Beckerman, B., DeLuca, P., Finkelstein, N., Ito, K., Moore, D. K., Newbold, K. B., Ramsay, T., Ross, Z., Shin, H., and Tempalski, B.: Extended follow-up and spatial analysis of the American Cancer Society study linking particulate air pollution and mortality, Res Rep Health Eff Inst, 5-114; discussion 115-136, 2009.

Lelieveld, J., Barlas, C., Giannadaki, D., and Pozzer, A.: Model calculated global, regional and megacity premature mortality due to air pollution, Atmospheric Chemistry and Physics, 13, 7023-7037, 2013.

Levy, I.: A national day with near zero emissions and its effect on primary and secondary pollutants, Atmospheric Environment, 77, 202-212, https://doi.org/10.1016/j.atmosenv.2013.05.005, 2013.

Li, K., Jacob, D. J., Liao, H., Shen, L., Zhang, Q., and Bates, K. H.: Anthropogenic drivers of 2013–2017 trends in summer surface ozone in China, Proceedings of the National Academy of Sciences, 116, 422-427, 10.1073/pnas.1812168116, 2019.

Li, M., Zhang, Q., Kurokawa, J. I., Woo, J. H., He, K., Lu, Z., Ohara, T., Song, Y., Streets, D. G., Carmichael, G. R., Cheng, Y., Hong, C., Huo, H., Jiang, X., Kang, S., Liu, F., Su, H., and Zheng, B.: MIX: a mosaic Asian anthropogenic emission inventory under the international collaboration framework of the MICS-Asia and HTAP, Atmos. Chem. Phys., 17, 935-963, 10.5194/acp-17-935-2017, 2017.

Li, T., Yan, M., Ma, W., Ban, J., Liu, T., Lin, H., and Liu, Z.: Short-term effects of multiple ozone metrics on daily mortality in a megacity of China, Environmental Science and Pollution Research, 22, 8738-8746, 2015.

Li, Y., Lau, A. K. H., Fung, J. C. H., Zheng, J., Zhong, L., and Louie, P. K. K.: Ozone source apportionment (OSAT) to differentiate local regional and super-regional source contributions in the Pearl River Delta region, China, Journal of Geophysical Research, 117, 2012a.

Li, Y., Lau, A. K. H., Fung, J. C. H., Zheng, J. Y., Zhong, L. J., and Louie, P. K. K.: Ozone source apportionment (OSAT) to differentiate local regional and super-regional source contributions in the Pearl River Delta region, China, Journal of Geophysical Research: Atmospheres, 117, D15305, 10.1029/2011JD017340, 2012b.

Lim, S. S., Vos, T., Flaxman, A. D., Danaei, G., Shibuya, K., Adairrohani, H., Almazroa, M. A., Amann, M., Anderson, H. R., and Andrews, K. G.: A comparative risk assessment of burden of disease and injury attributable to 67 risk factors and risk factor clusters in 21 regions, 1990-2010: a systematic analysis for the Global Burden of Disease Study 2010, The Lancet, 380, 2224-2260, 2012.

Liu, H., Liu, S., Xue, B., Lv, Z., Meng, Z., Yang, X., Xue, T., Yu, Q., and He, K.: Ground-level ozone pollution and its health impacts in China, Atmospheric Environment, 173, 223-230, https://doi.org/10.1016/j.atmosenv.2017.11.014, 2018a.

Liu, Y. H., Ma, J. L., Li, L., Lin, X. F., Xu, W. J., and Ding, H.: A high temporal-spatial vehicle emission inventory based on detailed hourly traffic data in a medium-sized city of China, Environ Pollut, 236, 324-333, 10.1016/j.envpol.2018.01.068, 2018b.

Lu, X., Hong, J., Zhang, L., Cooper, O. R., Schultz, M. G., Xu, X., Wang, T., Gao, M., Zhao, Y., and Zhang, Y.: Severe Surface Ozone Pollution in China: A Global Perspective, Environmental Science & Technology Letters, 5, 487-494, 10.1021/acs.estlett.8b00366, 2018.

National: National Health and Family Planning Commission of China, https://www.yearbookchina.com/navibooklist-n3018112802-1.html, in, 2018.

National Bureau of Statistics of China: http://www.stats.gov.cn/tjsj/pcsj/rkpc/6rp/indexch.htm., 2010.

Pudasainee, D., Sapkota, B., Bhatnagar, A., Kim, S., and Seo, Y.: Influence of weekdays, weekends and bandhas on surface ozone in Kathmandu valley, Atmospheric Research, 95, 150-156, 2010.

Pusede, S. E., Steiner, A. L., and Cohen, R. C.: Temperature and recent trends in the chemistry of continental surface ozone, Chemical reviews, 115, 3898-3918, 2015.

Sillman, S.: The use of NOy , H2O2, and HNO3 as indicators for ozone-NOx-hydrocarbon sensitivity in urban locations, Journal of Geophysical Research: Atmospheres, 100, 14175-14188, 10.1029/94jd02953, 1995.

Sillman, S., and He, D.: Some theoretical results concerning O3-NOx-VOC chemistry and NOx-VOC indicators, Journal of Geophysical Research, 107, 2002.

Streets, D. G., Bond, T. C., Carmichael, G. R., Fernandes, S. D., Fu, Q., He, D., Klimont, Z., Nelson, S. M., Tsai, N. Y., Wang, M. Q., Woo, J. H., and Yarber, K. F.: An inventory of gaseous and primary aerosol emissions in Asia in the year 2000, Journal of Geophysical Research: Atmospheres, 108, 10.1029/2002JD003093, 2003.

Tan, P.-H., Chou, C., and Chou, C. C. K.: Impact of urbanization on the air pollution “holiday effect” in Taiwan, Atmospheric Environment, 70, 361-375, https://doi.org/10.1016/j.atmosenv.2013.01.008, 2013.

Tan, P., Chou, C., Liang, J., Chou, C. C. K., and Shiu, C.: Air pollution "holiday effect" resulting from the Chinese New Year, Atmospheric Environment, 43, 2114-2124, 2009.

Wang, J., Ho, S. S. H., Cao, J., Huang, R., Zhou, J., Zhao, Y., Xu, H., Liu, S., Wang, G., Shen, Z., and Han, Y.: Characteristics and major sources of carbonaceous aerosols in PM2.5 from Sanya, China, Science of The Total Environment, 530-531, 110-119, https://doi.org/10.1016/j.scitotenv.2015.05.005, 2015.

Wang, J., Zhao, B., Wang, S., Yang, F., Xing, J., Morawska, L., Ding, A., Kulmala, M., Kerminen, V.-M., Kujansuu, J., Wang, Z., Ding, D., Zhang, X., Wang, H., Tian, M., Petäjä, T., Jiang, J., and Hao, J.: Particulate matter pollution over China and the effects of control policies, Science of The Total Environment, 584-585, 426-447, https://doi.org/10.1016/j.scitotenv.2017.01.027, 2017a.

Wang, P., Chen, Y., Hu, J., Zhang, H., and Ying, Q.: Attribution of Tropospheric Ozone to NOx and VOC Emissions: Considering Ozone Formation in the Transition Regime, Environmental Science & Technology, 53, 1404-1412, 10.1021/acs.est.8b05981, 2019a.

Wang, P., Chen, Y., Hu, J., Zhang, H., and Ying, Q.: Source apportionment of summertime ozone in China using a source-oriented chemical transport model, Atmospheric Environment, 211, 79-90, https://doi.org/10.1016/j.atmosenv.2019.05.006, 2019b.

Wang, P., Wang, T., and Ying, Q.: Regional source apportionment of summertime ozone and its precursors in the megacities of Beijing and Shanghai using a source-oriented chemical transport model, Atmospheric Environment, 224, 117337, https://doi.org/10.1016/j.atmosenv.2020.117337, 2020a.

Wang, T., Xue, L., Brimblecombe, P., Lam, Y. F., Li, L., and Zhang, L.: Ozone pollution in China: A review of concentrations, meteorological influences, chemical precursors, and effects, Science of The Total Environment, 575, 1582-1596, https://doi.org/10.1016/j.scitotenv.2016.10.081, 2017b.

Wang, Y., Wild, O., Chen, X., Wu, Q., Gao, M., Chen, H., Qi, Y., and Wang, Z.: Health impacts of long-term ozone exposure in China over 2013–2017, Environment International, 144, 106030, https://doi.org/10.1016/j.envint.2020.106030, 2020b.

Wang, Z., Chen, Y., Su, J., Guo, Y., Zhao, Y., Tang, W., Zeng, C., and Chen, J.: Measurement and Prediction of Regional Traffic Volume in Holidays, 2019 IEEE Intelligent Transportation Systems Conference, ITSC 2019, 2019c, 486-491.

Wiedinmyer, C., Akagi, S., Yokelson, R. J., Emmons, L., Al-Saadi, J., Orlando, J., and Soja, A.: The Fire INventory from NCAR (FINN): a high resolution global model to estimate the emissions from open burning, Geoscientific Model Development, 4, 625, 2011.

Xu, Z., Huang, X., Nie, W., Chi, X., Xu, Z., Zheng, L., Sun, P., and Ding, A.: Influence of synoptic condition and holiday effects on VOCs and ozone production in the Yangtze River Delta region, China, Atmospheric Environment, 168, 112-124, https://doi.org/10.1016/j.atmosenv.2017.08.035, 2017.

Yin, P., Chen, R., Wang, L., Meng, X., Liu, C., Niu, Y., Lin, Z., Liu, Y., Liu, J., and Qi, J.: Ambient Ozone Pollution and Daily Mortality: A Nationwide Study in 272 Chinese Cities, Environmental Health Perspectives, 125, 117006, 2017.

Zhang, H., Li, J., Ying, Q., Yu, J. Z., Wu, D., Cheng, Y., He, K., and Jiang, J.: Source apportionment of PM2.5 nitrate and sulfate in China using a source-oriented chemical transport model, Atmospheric Environment, 62, 228-242, https://doi.org/10.1016/j.atmosenv.2012.08.014, 2012.

Zhang, Q., Streets, D. G., He, K., Wang, Y., Richter, A., Burrows, J. P., Uno, I., Jang, C. J., Chen, D., Yao, Z., and Lei, Y.: NOx emission trends for China, 1995–2004: The view from the ground and the view from space, Journal of Geophysical Research: Atmospheres, 112, 10.1029/2007JD008684, 2007.

Zhao, J., Cui, J., Zhang, Y., and Luo, T.: Impact of holiday-free policy on traffic volume of freeway: An investigation in Xi'an, in: 8th International Conference on Green Intelligent Transportation Systems and Safety, 2017, edited by: Wang, W., Jiang, X., and Bengler, K., Springer Verlag, 117-124, 2019.